Preparation and characterization of chloroaluminum phthalocyanine-loaded solid lipid nanoparticles by thermal analysis and powder X-ray diffraction techniques

Ellen Denise P. Almeida · Adjane A. Costa · Mairim R. Serafini ·
Fábia C. Rossetti · Juliana M. Marchetti · Victor Hugo V. Sarmento ·
Rogéria de S. Nunes · Mário Ernesto G. Valerio · Adriano A.S. Araújo ·
Ana Amélia M. Lira

Abstract Solid lipid nanoparticles (SLN) without drug and SLN loaded with chloroaluminum phthalocyanine (AlClPc) were prepared by solvent diffusion method in aqueous system and characterized by thermal analyses and X-ray diffraction (XRD) in this study. Determination of particle size, zeta potential (ZP), and encapsulation efficiency were also evaluated. SLN containing AlClPc of nanometer size with high encapsulation efficiency and ZP were obtained. The results indicated that the size of SLN loaded with AlClPc is larger than that of the inert particle, but ZP is not changed significantly with incorporation of the drug. In differential scanning calorimetry (DSC) curves, it was observed that the melting point of stearic acid (SA) isolated and in SLN occurred at 55 and 64 °C, respectively, suggesting the presence of different polymorphs. DSC also shows that the crystallinity state of SLN was much less than that of SA isolated. The incorporation of drug in SLN may have been favored by this lower crystallinity degree of the samples. XRD techniques corroborated with the thermal analytic techniques, suggesting the polymorphic modifications of stearic acid.

Keywords Chloroaluminum phthalocyanine · Solid lipid nanoparticles · Thermal analysis · X-ray diffraction

Introduction

Photodynamic therapy is a non-surgical, minimally invasive approach, which has been used in the treatment of superficial epithelial tumors such as oral squamous carcinomas and non-melanoma skin cancer [1–3]. The therapy is based on the photoactivation of a photosensitizer (PS) when irradiated by light in a specific wavelength window (generally the maximum absorption band of the PS compound). The light-excited PS generates reactive oxygen species (ROS) that induce reduction or destruction of tumors by multifactorial mechanisms [4].

Among the various PS drugs investigated, phthalocyanines have been found to be highly promising [1, 2, 5]. Phthalocyanines present a variety of metal ions in their chemical structure, which are indeed responsible for the particular property of each molecule. Aluminum (III) is a metal ion used for enhancing phthalocyanine phototoxicity [2, 6]. However, most phthalocyanines are hydrophobic compounds requiring association to specific drug delivery systems for clinical use.

Solid lipid nanoparticles (SLN) are alternative colloidal carrier systems for controlled drug delivery with a mean diameter between approximately 50 and 1,000 nm, which presents some advantages when compared with other particulate carriers, such as a good tolerability and biodegradation, a high bioavailability, a targeting effect, encapsulation of a poorly water soluble drug, and no

E. D. P. Almeida · A. A. Costa · M. R. Serafini ·
R. de S. Nunes · A. A.S.Araújo · A. A. M. Lira (✉)
Departamento de Fisiologia, Universidade Federal de Sergipe,
Av. Marechal Rondon, s/n, Cidade Universitária, São Cristóvão
49000-100, Sergipe, Brazil
e-mail: ana_lira2@hotmail.com

F. C. Rossetti · J. M. Marchetti
Faculdade de Ciências Farmacêuticas de Ribeirão Preto,
Universidade de São Paulo, Ribeirão Preto, Brazil

V. H. V. Sarmento
Departamento de Química, Universidade Federal de Sergipe,
Itabaiana, Brazil

M. E. G. Valerio
Departamento de Física, Universidade Federal de Sergipe,
São Cristóvão, Brazil

problems with respect to large scale production and sterilization [7, 8]. However, as for all drug delivery systems, detailed characterization is a major part of the research and development work on lipid nanoparticle dispersions to ensure the generation of systems with the desired properties. Among several analytic techniques employed for this purpose, differential scanning calorimetry (DSC) and X-ray diffraction (XRD) play a prominent role because they are able to provide structural information on the dispersed particles, and they have been employed to investigate the crystalline structure of SLN and the drug [9–12]. Moreover, the use of these two techniques often leads to complementary information on the systems of interest.

The aim of this study was to prepare chloroaluminum phthalocyanine (AlClPc)-loaded SLN for photodynamic therapy of non-melanoma skin cancer using stearic acid (SA) as solid lipid and to characterize these systems by DSC, TG/DTG, and XRD techniques. Particle size, entrapment efficiency (EE), drug loading (DL), and zeta potential (ZP) of SLN were also evaluated.

Materials and methods

Materials

AlClPc was acquired from Aldrich Chemical Company. SA was purchased from VETEC (Brazil). All the other solvents and reagents obtained were of analytic grade.

Preparation of SLN

SLN containing AlClPc and inert SLN (without drug) were prepared by solvent diffusion technique in an aqueous system using SA as solid lipid according to the modified method earlier described by Hu et al. [13]. In brief, SA and drug (AlClPc) were completely dissolved in ethanol (3 mL) in a water bath at 70 °C. The resultant organic solution was quickly dispersed into 120 mL of sodium lauryl sulfate (SDS) aqueous solution (2%, w/w) warmed to 70 °C under magnetic stirring. The obtained

pre-emulsion (melted lipid droplet) was then cooled at room temperature until drug-loaded SLN dispersion was obtained. After 24 h, under continual stirring for solvent evaporation, SLN was cooled to 4 °C to enable aggregation of nanoparticles. The aggregate of nanoparticle dispersion was then centrifuged (5,000 rpm for 1 h to 4 °C, 5804R Model, Eppendorf). The precipitate of SLN was redispersed into SDS aqueous solution (0.2%, w/w) to remove the drug adsorbed on the surface of lipid nanoparticles. Then, the AlClPc-SLN was collected by centrifugation at 5,000 rpm for 15 min, the precipitate was frozen, and then the sample was moved to the freeze–drier. SLN prepared with drug:lipid at different proportions w/w were obtained (Table 1). Inert SLN were prepared by the same procedure.

Determination of particle size and zeta potential

The particle size and ZP of the resulting AlClPc-SLN were measured by Zetasizer (Malvern Instruments, UK). For the preparation of samples, the SLN dispersions were diluted 30 times with distilled water.

Determination of drug entrapment efficiency (EE) and drug loading (DL)

The contents of AlClPc in the two supernatants, removed as mentioned in the method of SLN preparation, were measured by fluorescence spectroscopic technique. First, supernatant was separated after the SLN dispersion was centrifuged. Another supernatant was separated after the SLN were washed by 0.2% SDS solution (w/w) and centrifuged again. The drug EE and DL of AlClPc-loaded SLN were then calculated from formulas 1 and 2:

$$DL = \frac{(WT - WS1 - WS2)}{(WT - WS1 - WS2 - WL)} \times 100\% \tag{1}$$

$$EE = \frac{(WT - WS1 - WS2)}{(WT)} \times 100\% \tag{2}$$

where WT was the total amount of charged drug. The drug content in aqueous solution was taken into account in the calculation of the EE and DL of SLN. WS1 was the amount

Table 1 Particle size, polydispersity index (PDI), entrapment efficiency (EE), drug loading (DL), and zeta potential (ZP) of stearic acid (SA) in SLN

SLN	AlClP/mg	Stearic acid/mg	SDS/w/w%	Entrapment efficiency/%	Drug loading/%	Size/nm	Zeta potential/mV	PDI
Inert SLN	–	190	2	–	–	142.7	−54.8	0.49
SLN 1	5	100	2	79.01	4.75	639.3	−50.7	0.79
SLN 2	5	190	2	85.78	2.50	255.1	−57.0	0.67
SLN 3	5	250	2	71.61	1.96	218.9	−56.8	0.48

SDS sodium lauryl sulfate

of drug in the supernatant after the first centrifugation, WS2 was the amount of drug in the supernatant after the second centrifugation, and WL was the total amount of charged lipid [14].

The quantification of AlClPc encapsulated was carried out according to a validated methodology based in fluorescence spectroscopic technique. Samples were excited at 375 nm, and the AlClPc concentrations were measured from the standard curve. Linearity was achieved over the concentration range between 0.01 and 0.2 μg/mL, presenting a correlation coefficient (R) of 0.998. These values are considered adequate for an analytic method. Parameters such as precision, accuracy, and limit of quantification were also evaluated.

Thermal analysis

DSC curves of pure SA, inert SLN, isolated drug, and AlClPc-loaded SLN were obtained in a DSC-50 cell (Shimadzu) using aluminum crucibles with samples of about 2 mg, under dynamic nitrogen atmosphere (50 mL/min) and heating rate of 10 °C/min in the temperature range from 25 to 600 °C. The DSC cell was calibrated with indium (m.p. 156.6 °C; $\Delta H_{\text{fus.}} = 28.54$ J/g), conforming to ASTM standards [15].

TG/DTG curves of pure stearic acid, inert SLN, AlClPc, and AlClPc-loaded SLN were obtained with a thermobalance model TGA 50 (Shimadzu) in the temperature range of 25–900 °C, using platinum crucibles with samples of about 3 mg, under dynamic nitrogen atmosphere (50 mL/min) and heating rate of 10 °C/min. The TG/DTG was calibrated with calcium oxalate monohydrate, conforming to ASTM standards.

X-ray diffraction

X-ray diffraction measurements were performed to clearly elucidate the solid state of lipid and drug in SLN using an X-ray diffractometer (Rigaku, Rint/2000 Model). The X-ray diffractogram was scanned with the diffraction angle increasing from 3 to 40°, 2θ angle, at speed 2°/min, and at a constant temperature of 25 °C.

Results and discussion

Particle size and zeta potential

The SLN were characterized to assess the effect of the different proportions of lipid and drug on mean particle size, size distribution, and surface charge. The particle size and polydispersity index (PDI) of the SLN obtained are reported in Table 1. It was possible to obtain submicronsized SLN with all lipid:drug proportions. In fact, SLN showed a mean diameter in the range of 142–639 nm. The PDI value was in the range of 0.48–0.79 for all the SLN investigated. These values can be considered high for use on routes, such as parenteral, but are acceptable for topical applications. There was an increase in particle size when formulated with AlClPc. Inert SLN presented a mean diameter of about 142 nm, while SLN containing AlClPc presented mean diameters in the range of 218–639 nm. Hu et al. [13, 16] found similar results for SA in the SLN, where incorporation of a lipophilic model drug, Clobetasol Propionate, resulted in a significantly increased size of the SLN studied.
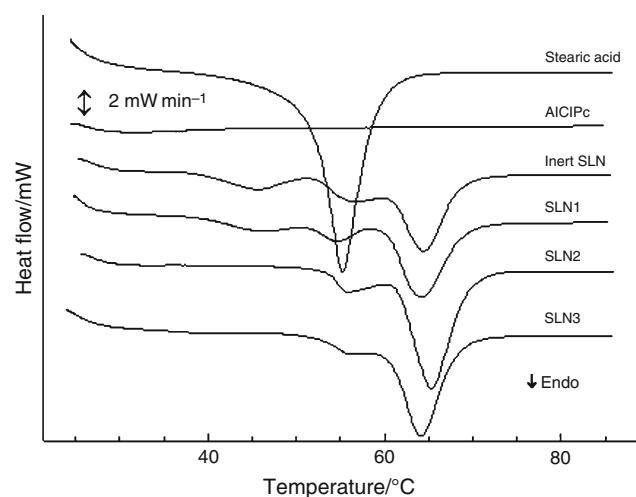
Zeta potential (ZP) can make a prediction about the stability of colloid dispersions. A high ZP ($>\pm30$ mV) can provide an electric repulsion to avoid the aggregation of particles [16, 17]. The ZPs of the SLN obtained are also listed in Table 1. The incorporation of AlClPc into lipid nanoparticles had weak influence on the ZP of the particles, which was about −50 mV in all the cases. This demonstrates that the nanoparticle dispersion obtained by solvent diffusion method in an aqueous system is a physically stable system in this study.

Drug entrapment efficiency and drug loading

Table 1 also shows the results of entrapment efficiency (EE) and DL for the SLN obtained. The EE and DL of SLN were from 71 to 85% and from 1.96 to 4.75%, respectively. Several authors correlate the encapsulation efficiency with the crystallinity degree of the samples. Previous studies have shown that the greater the disorganization of the crystalline matrix of the system obtained, the greater the drug encapsulation ability [9, 13, 18]. Thus, techniques of thermal analysis and X-ray diffraction were employed to evaluate these changes.

An important point to be considered in the characterization of SLN is the potential occurrence of different polymorphic forms [19]. The different molecular packing in the polymorphic modifications is reflected in differences of physical properties like the melting points and enthalpies. In general, the production process of the nanoparticles can change the type of polymorph [9, 19]. Fatty acids like SA, which are usually employed for the preparation of the corresponding systems, can exist in four different polymorphic forms namely A, B, C, and E [20, 21]. All these forms can be obtained upon crystallization from solution, but it is believed that only the C form grows upon crystallization from the melt. This form has also been found with DSC and X-ray diffraction in (dried) SA nanoparticle preparations [9, 22, 23].

Then, SA, AlClPc, and SLN obtained in this study were analyzed by DSC and TG/DTG (Figs. 1 and 2). Table 2 shows the corresponding DSC data for the melting point of SA. To produce SLN, the lipid is melted, the drug is dissolved in the melted lipid, and then this drug-containing melt is dispersed in a hot surfactant solution to yield a pre-emulsion. Cooling leads to crystallization of the lipid and formation of SLN. The melting point of SA was 55 °C for isolated solid lipid close to the event mentioned in the literature for polymorph B (54 °C) [24]. In order to differentiate between the actual effect of the SLN production process and the effect of the AlClPc, inert SLN (without drug) were also prepared and analyzed. According to data presented in Fig. 1 and Table 2, crystallization of SLN during the preparation method promoted a polymorphic modification of the lipid particle matrix. The melting point
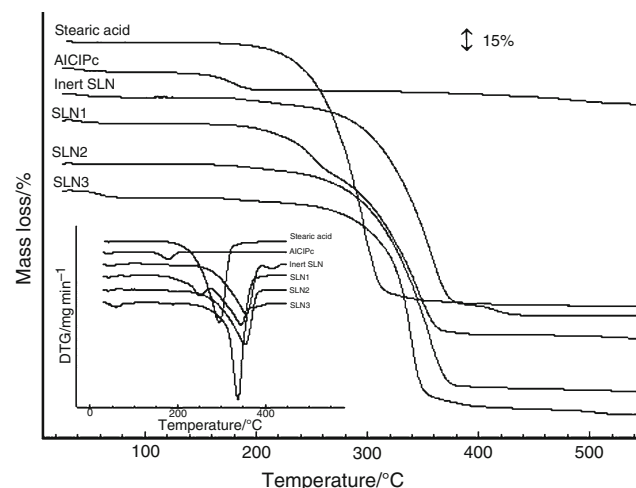
Table 2 Onset temperature, melting point (peak maximum), and melting enthalpy of stearic acid in SLN with and without drug

SLN	Peak maximum/°C	T_{onset}/°C	Melting enthalpy/J/g
Stearic acid	55.6	47.3	−167.2
Inert SLN	64.3	59.5	−48.0
SLN 1	64.1	58.5	−47.2
SLN 2	65.3	60.0	−77.2
SLN 3	64.0	58.5	−65.6

Fig. 1 DSC curves of AlClPc, SA, inert SLN, AlClPc-loaded SLN in dynamic nitrogen (50 mL/min), and heating rate of 10 °C/min

Fig. 2 TG/DTG curves of AlClPc, SA, inert SLN, AlClPc-loaded SLN in dynamic nitrogen (50 mL/min), and heating rate of 10 °C/min

temperature of SA in inert SLN was shifted to the temperature of 64 °C, suggesting the presence of C polymorph, which is thermodynamically the most stable form and may be obtained by solidification of the melt and sometimes by crystallization from a polar solvent [22, 24]. Garti et al. [24] also showed that the crystallization of SA from a non-polar solvent usually gives either the A form or a mixture of the B and C forms. Moreover, Aquilano et al. [22] showed that solid liposheres prepared with SA, co-surfactant (solvent), and surfactant has resulted in the formation of C polymorph, although B polymorph was also present in some samples. The presence of B polymorph was dependent on the concentration of co-surfactant used (butanol). In Fig. 1, it is observed that C polymorph is present predominantly in all the nanoparticle samples (64 °C). Figure 1 shows another event at 55 °C for all the SLN, and one event at 45 °C for inert SLN and SLN 1. Compared to the literature data, these events seem to correspond to phase transition of B polymorph and dehydration (water associated to nanoparticles), respectively [24]. This dehydration is also shown in the TG/DTG curve (Fig. 2) where a water loss was verified for all the SLN.

It is also seen in Table 2 that the enthalpy of SA in the SLN was reduced relative to that of lipid alone. As a result, it can be concluded that the lipid within the nanoparticles presented lower crystallinity degree compared with pure SA. Several factors can influence the crystallinity degree, such as lyophilization and the presence of drug and surfactant [18, 25]. Li et al. [18] observed that there was a sharp decline in the enthalpy from the pure lipid to the nanoparticles. For less-ordered crystals or amorphous solids, the melting of the substance requires much less energy than crystalline substances that need to overcome lattice forces. Thus, those authors concluded that the lipid within the nanoparticles should be in a less-ordered arrangement when compared to the pure lipid. This can indicate that the crystallinity degree of lipid matrix in SLN was lower than that of SA isolated.

On comparing the DSC curves obtained from inert SLN with AlClPc-loaded SLN, it can be observed that the concentration of drug and of SA in relation to SDS solution

affected the enthalpy and, consequently, the crystallinity degree. In general, the crystallinity degree of the lipid matrix in SLN provides useful information about its behavior in the incorporation of drugs. That is, an ideal formulation of SLN should present a lower degree of crystallinity, increasing the DL and avoiding the drug expulsion after melting and recrystallization [18]. A high value of enthalpy of fusion suggests high organization in the crystal lattice because the fusion of a highly organized crystal requires more energy to overcome the forces of cohesion in the crystal lattice than that is required in a crystal less ordered or amorphous [18].

Indeed, SLN with the highest DL also had lesser enthalpy and a lower degree of crystallinity, and seem to be the most appropriate delivery system for incorporating AlClPc. Hu et al. [13] also found similar results for lipid nanoparticles of SA containing clobetasol propionate. However, the highest enthalpy and melting point was for SLN 2, which presents a DL of 2.5% at the concentration of 190 mg of SA in 120 mL of 2% SDS solution (w/w). This suggests that the final proportion of SA and surfactant (SDS) in lyophilized nanoparticles (amount of impurity) also significantly influences the degree of crystallinity of the samples.

TG curve of SA (Fig. 2) showed two events of mass loss relative to the thermal decomposition ($T_{peak\ DTG} = 296.9$ °C e $\Delta m = 95.13\%$) followed by elimination of carbonaceous material. AlClPc presented a thermal event at 157.2 °C in DSC curve, which was accompanied by a mass loss ($\Delta m = 6.2\%$) observed by TG/DTG curves probably because of volatiles evaporation (N_2, O_2, CO_2, and H_2O) or low-temperature degradation of unstable chemical fragments in the samples. Inert SLN showed a two-step mass loss. The first event occur $T_{peak\ DTG} = 359.3$ °C corresponding the loss of $\Delta m = 75.1\%$; in the second event $T_{peak\ DTG} = 416.5$ °C is observed a mass loss of $\Delta m = 3.81\%$.

As shown in Fig. 2, the mass loss (%) of free SLN 1 at the heating rate of 10 °C/min can be divided into four consecutive processes. The sample in first stage is in the temperature range from 25 to 80 °C with a Δm of 1.0%, which is due to the release of water molecules from the outside or/and inside of nanoparticles. Subsequently, the sample in the second stage is kept in a very wide temperature range, i.e., from 177.7 to 265.1 °C ($\Delta m = 17.6\%$). Then, the sample in the third stage undergoes a rapid decomposition ($\Delta m = 58.76\%$). During continuous heating, the sample in the last stage is carbonized ($\Delta m = 1.7\%$). Thermal behaviors of the SLN 2 and SLN 3 were very similar to each other. TG curves presented a characteristic profile of elimination of water surface between 35 and 80 °C, with thermal stability between 100 and 160 °C, following thermal decomposition with carbonization.

X-ray diffraction (XRD) was employed to investigate the crystalline structure of SLN and the drug. Diffractograms of SLN, AlClPc, and SA are displayed in Fig. 3. The diffraction curve of SA shows differences from those of SLN. Compared with the pure lipid, the peak intensities of SLN without drug are much weaker, which indicates that the SA is presented in a less crystalline form in these samples. Thus, the results seem to indicate that SA in SLN was partially recrystallized or less ordered, as observed previously by the DSC. The diffractograms of SA exhibit sharp peaks at 2θ scattered angles of 7.07, 20.60, 21.71, and 24.05°, indicating the lipid crystalline nature. The diffractograms of inert SLN exhibit small peaks at 2θ scattered angles of 6.48, 20.97, 21.71, 22.23, and 24.12°, showing some different XRD patterns (Fig. 3). These changes are because of the presence of a mixture of polymorphs in the nanoparticles and the method of obtaining the SLN. It can also be seen that the diffractograms of SLN after the addition of AlClPc had minor changes. The diffractograms of SLN containing drug exhibited small peaks at 2θ scattered angles of 6.56, 21.04, 22.06, and 24.19° for SLN 1; 6.56, 21.08, 21.59, 22.09, and 24.12° for SLN 2; and 6.56, 21.12, 21.63, 22.21, and 24.19° for SLN 3. The low intensity of peaks makes it difficult to distinguish events related to each polymorph, compared to the available data in the literature. Also, peaks of AlClPc could not be observed in these diffractograms. Compared with the pure lipid, the peak intensities of SLN are much weaker, which indicates that the SA is presented in a less crystalline form in these samples. Thus, the results seem to indicate that SA in SLN was partially recrystallized or less ordered, as observed previously by the DSC and TG/DTG.

Combining the DSC and XRD data, it can be concluded that there was a change in the crystalline structure of SA in
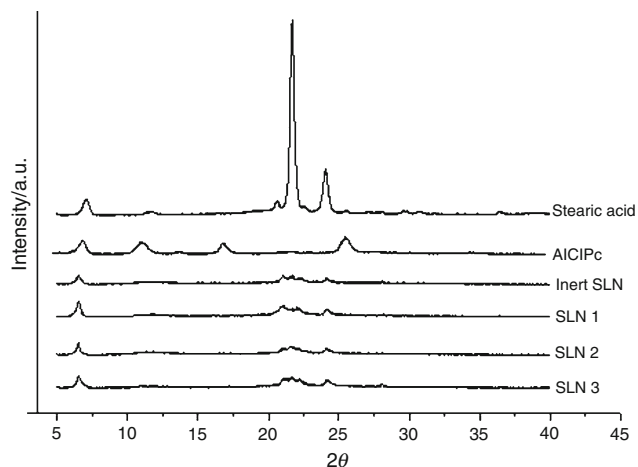
Fig. 3 X-ray diffractograms of AlClPc, SA, inert SLN, and AlClPc-loaded SLN

the SLN, suggesting polymorphic modification of the lipid particle matrix. Besides this, the method of production of SLN did not favor the total crystallization of the samples, which may be related to the high encapsulation efficiency obtained.

Conclusions

Solvent diffusion technique was successfully employed to prepare the SLN. The experimental results reveal that drug-loaded SLN presented nanometer size and high encapsulation efficiency, and ZP. DSC and XRD experiments showed that there was a change in the crystalline structure of SA in the SLN, suggesting polymorphic modification. The lipid in SLN is also less ordered, and the lower crystallinity degree of the lipid matrix seems to be related to the high encapsulation efficiency obtained.

References

1. Longo JPF, Lozzi SP, Simioni AR, Morais PC, Tedesco AC, Azevedo RB. Photodynamic therapy with aluminum-chlorophtalocianine induces necrosis and vascular damage in mice tongue tumors. J Photochem Photobiol B Biol. 2009;94:143–6.
2. Tapajós EC, Longo JP, Simionim AR, Lacava ZG, Santos MF, Morais PC, Tedesco AC, Azevedo RB. In vitro photodynamic therapy on human oral keratinocytes using chloroaluminum–phthalocyanine. Oral Oncol. 2008;44:1073–9.
3. Lopez RFV, Lange N, Guy R, Bentley MVL. Photodynamic therapy of skin cancer: controlled drug deliveryof 5-ALA and its esters. Adv Drug Deliv Rev. 2004;13:77–9.
4. Allison RR, Downie GH, Cuenca R, Hu XH, Childs CJH, Sibata CH. Photosensitizers in clinical PDT. Photodiagn Photodyn Ther. 2004;1:27–42.
5. Ricci-Júnior E, Marchetti JM. Zin (II) phtalocyanine loaded PLGA nanoparticles for photodynamic therapy use. Int J Pharm Amsterdam. 2006;310:187–95.
6. Nunes SMT, Sguilla FS, Tedesco AC. Photophysical studies of zinc phthalocyanine and chloroaluminum phthalocyanine incorporated into liposomes in the presence of additives. Braz J Med Biol Res. 2004;37:273–84.
7. Chen H, Chang X, Du D, et al. Podophyllotoxin-loaded solid lipid nanoparticles for epidermal targeting. J Control Release. 2006;110:296–306.
8. Li Y, Dong L, Jia A, et al. Preparation and characterization of solid lipid nanoparticles loaded traditional chinese medicine. Int J Biol Macromol. 2006;38:296–9.
9. Bunjes H, Unruh T. Characterization of lipid nanoparticles by differential scanning calorimetry, X-ray and neutron scattering. Adv Drug Del Rev. 2007;59:379–402.
10. Nunes PS, Bezerra MS, Costa LP, Cardoso JC, Albuquerque RLC Jr, Rodrigues MO, Barin GB, Silva FA, Araújo AAS. Thermal characterization of usnic acid/collagen-based films. J Therm Anal Calorim. 2010;99:1011–4.
11. Cardoso JC, Albuquerque RLC Jr, Padilha FF, Bittencourt FO, Freitas O, Nunes PS, Pereira NL, Fonseca MJV, Araújo AAS. Effect of the Maillard reaction on properties of casein and casein films. J Therm Anal Calorim. 2011;104:249–54.
12. Brito MB, Barin GB, Araújo AAS, Sousa DP, Cavalcanti SCH, Lira AAM, Nunes RS. The action modes of Lippia sidoides (Cham) essential oil as penetration enhancers on snake skin. J Therm Anal Calorim. 2009;97(1):323–7.
13. Hu FQ, Jiang SP, Du YZ, Yuan H, Ye YQ, Zeng S. Preparation and characterization of stearic acid nanostructured lipid carriers by solvent diffusion method in an aqueous system. Col Surf B Bioint. 2005;45:167–73.
14. Hu FQ, Zhang Y, Zhong Du Y, Yuan H. Nimodipine loaded lipid nanospheres prepared by solvent diffusion method in a drug saturated aqueous system. Int J Pharm. 2008;348:146–52.
15. Lira AAM, Nanclares DMA, Federman NA, Marchetti JM. Drug: polymer interaction in the all-trans retinoic acid release from chitosan microparticles. J Therm Anal Cal. 2007;87:899–903.
16. Hu FQ, Yuan H, Zhang HH, Fang M. Preparation of solid lipid nanoparticles with clobetasol propionate by a novel solvent diffusion method in aqueous system and physicochemical characterization. Int J Pharm. 2002;239:121–8.
17. Komatsu H, Kitajima A, Okada S. Pharmaceutical characterization of commercially available intravenous fat emulsions: estimation of average particle size, size distribution and surface potential using photon correlation spectroscopy. Chem Pharm Bull. 1995;43:1412–5.
18. Li Z, Yu L, Zheng L, Geng F. Studies on crystallinity state of puerarin loaded solid lipid nanoparticles prepared by double emulsion method. J Therm Anal Calorim. 2010;99:689–93.
19. Müller RH, Runge SA, Ravelli V, et al. Cyclosporine-loaded solid lipid nanoparticles (SLN®): drug–lipid physicochemical interactions and characterization of drug incorporation. Eur J Pharm Biopharm. 2008;68:535–44.
20. Gandolfo FG, Bot A, Flöter E. Phase diagram of mixtures of stearic acid and stearyl alcohol. Thermochim Acta. 2003;404:9–17.
21. Teixeira ACT, Garcia AR, Ilharco LM, da Silva AMPSG, Fernandes AC. Phase behaviour of oleanolic acid, pure, mixed with stearic acid: interactions and crystallinity. Chem Phys Lipids. 2010;163:655–66.
22. Aquilano A, Cavalli R, Gasco MR. Solid lipospheres from hot microemulsions in the presence of different concentrations of cosurfactant: the crystallization of stearic acid polymorphs. Thermochim Acta. 1993;230:29–37.
23. Cavalli R, Aquilano D, Carlotti ME, Gasco MR. Study by X-ray powder diffraction and differential scanning calorimetry of two model drugs, phenothiazine and nifedipine, incorporated into lipid nanoparticles. Eur J Pharm Biopharm. 1995;41:329–33.
24. Garti N, Sarig S, Wellner E. Determination of the composition of mixtures of fatty acid polymorphs by DTA. Thermochim Acta. 1980;37:131–6.
25. Abdelwahed W, Degobert G, Stainmesse S, Fessi H. Freeze–drying of nanoparticles: formulation, process and storage considerations. Adv Drug Deliv Rev. 2006;58:1688–713.